

Scattering of orthopositronium off a helium atom

Arindam Basu,¹ Prabal K. Sinha,² and A. S. Ghosh¹

¹*Department of Theoretical Physics, Indian Association for the Cultivation of Science, 2A&B, Raja S. C. Mullick Road, Jadavpur, Calcutta 700032, West Bengal, India*

²*Department of Physics, Bangabasi College, 19, Rajkumar Chakraborty Sarani, Calcutta 700009, West Bengal, India*

(Received 10 October 2000; published 13 April 2001)

Scattering of orthopositronium off helium target has been investigated using close-coupling method in the energy range 0–110 eV. Two basis sets, (a) $\text{Ps}(1s) + \text{He}(1s^2, 1s2^1s, 1s2^1p)$ and (b) $\text{Ps}(1s,2p) + \text{He}(1s^2, 1s2^1s, 1s2^1p)$, have been employed to find the scattering parameters. Low-order phase shifts, scattering length, and elastic and excitation cross section up to $n=2$ are reported using close-coupling approximation. Total cross section is also given by adding other partial cross section and compared with available measured data and existing theoretical predictions. Our total cross section at zero energy is very close to the theoretical prediction of Drachman and Houston [J. Phys B **3**, 1657 (1970)] and measured data of Canter *et al.* [Phys. Rev. A **12**, 375 (1975)]. Present total cross section is in qualitative agreement with measured data of the University College London group in the energy range considered. In particular, present predictions are in good agreement with the UCL group in the energy range 20–30 eV. It has been found that elastic cross section is dramatically reduced, at zero or near zero energies, with the inclusion of target excitation in the expansion scheme. Moreover, ionization cross section of the Ps atom is found to be a major contributor to the total cross section above the ionization threshold.

DOI: 10.1103/PhysRevA.63.052503

PACS number(s): 36.10.Dr, 34.50.-s

INTRODUCTION

We consider orthopositronium (*o*-Ps)-helium-atom scattering at low and intermediate energies. The importance of (*o*-Ps)-atom scattering was first realized by Massey and Mohr [1] who evaluated the first Born amplitude (FBA) using only the electron exchange interaction as direct FBA vanishes for the processes in which the initial and final states of the Ps atom have the same parity. Even for the simplest system, i.e., (*o*-Ps)-H, theoretical calculation is much more difficult than the corresponding electron (positron)-atom scattering. Added difficulty is due to the fact that both the atoms (Ps and H) have internal degrees of freedom and one has to encounter multiparticle and multicenter integrals. In the case of helium the situation is even worse.

Theoretically, study of (*o*-Ps)-He scattering has been initiated by Fraser [2,3] and Fraser and Kraidy [4] using the static exchange model, in which both the atoms are retained in their respective ground states while the effect of electron exchange is properly taken care of. Barker and Bransden [5,6] have investigated the same problem with and without the adiabatic part of van der Waals' potential. This lowest-order long-range potential is found to modify the scattering parameters. Drachman and Houston [7] have investigated (*o*-Ps)-He scattering and obtained the values of Z_{eff} and scattering length using a local exchange model potential. In this investigation they have included the effect of correlation by taking a close channel wave function having eighty-four independent terms and solved the problem by Kohn variational method. This paper is expected to provide meaningful results. The Belfast group [8] has applied the target-elastic pseudostate close-coupling method, neglecting the exchange of electrons between both the atoms, to study the problem in which the target helium atom always remains in its ground state. Sarkar and Ghosh [9] revisited the problem using static

exchange model for a wider range of energy. A three-state [$\text{Ps}(1s,2s,2p) + \text{He}(1s^2)$] target elastic CCA has been applied by Sarkar *et al.* [10]. The effect of electron exchange between the two atoms has been considered by antisymmetrizing the total wave function of the system. They have predicted elastic and Ps excitation (upto $n=2$) cross sections using target elastic CCA upto the incident Ps energy 200 eV. Recently, the Belfast group (Blackwood *et al.* [11]) has studied (*o*-Ps)-He scattering using target elastic coupled pseudostate (22 states) calculation in the energy range 0–40 eV. This is the most elaborate target elastic coupled channel calculation. Biswas and Adhikari [12] have also studied the problem using the close-coupling method in which the exchange of electrons between the projectile and target atoms has been represented by a tuned nonlocal model potential. Their predicted scattering parameters for *o*-Ps-He scattering differ significantly from all the other existing theoretical estimates.

The positronium atom is an exotic atom and has its own characteristics. The Ps atom is available both in spin triplet (ortho) and spin singlet (para) states. The lifetime of *o*-Ps is about 10^3 -fold longer than that of *p*-Ps. Consequently, *o*-Ps (ground state) which is sufficiently long lived, is used as a projectile for the scattering experiments. Due to the availability of monoenergetic energy tunable *o*-Ps beam [13], it is now possible to measure (*o*-Ps)-atom molecule scattering parameters in the laboratory. Measurements have already been carried out for total cross sections on Ps scattering off He, Ar, O₂, and H₂ targets using beam techniques [14–18]. In addition to these beam measurements, some cross section data have been deduced from observations of the annihilation rate of *o*-Ps in various gases at very low energies [19–21]. At very low energies, annihilation measurements correspond to momentum transfer cross section σ_m , which is given by

$$\sigma_m = \int (1 - \cos \theta) \frac{d\sigma_{el}}{d\Omega} d\Omega,$$

where $d\sigma_{el}/d\Omega$ is the elastic differential cross section. The σ_m at very low energy (near zero) may be considered to be the total cross section, since S -wave cross section is rather essentially the sole contributor to the total cross section at these energies.

The zero (or near zero) energy cross section data obtained so far by different experimental groups on (o -Ps)-He scattering differs dramatically among themselves. The largest cross section obtained by Nagashima *et al.* [19] is $13(\pm 4)\pi a_0^2$ using the beam technique, whereas, Skalsey *et al.* [22] measured the lowest value $2.6(\pm 0.5)\pi a_0^2$ using the time-dependent Doppler broadening spectroscopy. Theoretically, the situation is also not very much different. The highest theoretical cross section at zero (or near zero) energy is $14.584\pi a_0^2$ as predicted by Sarkar and Ghosh [9], while Biswas and Adhikari [12] obtained the lowest one as $2.7\pi a_0^2$. The UCL group has measured the total cross section for (o -Ps)-He scattering in the energy range 10–110 eV. The predicted values of Sarkar, Chaudhuri, and Ghosh [10] are in good agreement in the energy range 20–30 eV. The results of Blackwood *et al.* [11], who have performed the most elaborate calculation, are at variance with the measured data of the UCL group. However, except at the incident energy 10 eV, the results for total cross sections of Biswas and Adhikari [12] are in fair agreement with the measured data. Moreover, their total cross sections differ from all other theoretical predictions.

From the above discussion it is clear that, the total cross section at zero (or near zero) energy is an open question. Literature also reveals, at medium energies, the situations are also not very acceptable when comparison between measured data and theoretical predictions are made. We have noticed that the excitation and ionization cross sections of Ps atom contribute dominantly to the total cross section at these energies. The contributions, on the other hand, from the inelastic processes of the target atom is not very significant. Considering these, Blackwood *et al.* have performed an extensive calculation allowing inelastic processes of Ps atoms in their coupled pseudostate formalism. Below the first excitation threshold (5.1 eV), elastic cross section is the total cross section of the system. It has been found that the zero energy cross section changes very marginally from $14.584\pi a_0^2$ in the static exchange model [9] to $13.193\pi a_0^2$ in the 22-state target elastic coupled pseudostate method [11]. It is worth mentioning that the 22-state target elastic calculation incorporates, via pseudostates, the effect of higher excited states and continuum of the projectile atom. It is evident from the above discussion that the zero (or near zero) energy elastic cross section does not depend much on the virtual inelastic processes of the Ps atom. On the other hand, the calculations of Ray and Ghosh [23], Sinha, Basu, and Ghosh [24] and Basu *et al.* [25] on Ps-H scattering show that the low-energy elastic cross section reduce drastically, below the first excitation threshold, due to the inclusion of target inelastic channels. Moreover, Drachman and Houston [7]

have taken the correlation effect via their close channel wave function, which also includes the effect of the target inelastic channels. Their zero energy cross section is $7.73\pi a_0^2$, a change of about 41% when compared with the most elaborate target elastic CCA prediction of Blackwood *et al.* [11]. We would like to add further that Peach [26] as reported by the Belfast group [11], has included the effect of inelastic channels of the target atom through an adiabatic model potential and predicted a total cross section of about $3.3\pi a_0^2$ at zero energy. All these findings suggest that below the first excitation threshold of the system, target inelastic channels have to be considered to predict a good estimation to the cross section. It has been noticed, from the static exchange [9], three-state target elastic [10] and 22-state [11] calculations, that beyond the ionization threshold of the Ps atom, elastic cross section is reduced due to the loss of Ps inelastic flux. Further, van der Waals' interaction is supposed to play a vital role in determining the elastic cross section at low energies [5,6,24].

Based on the above discussion, we investigate Ps-He scattering using two basis sets:

$$(a) \text{Ps}(1s) + \text{He}(1s^2, 1s2^1s, 1s2^1p)$$

$$(b) \text{Ps}(1s,2p) + \text{He}(1s^2, 1s2^1s, 1s2^1p).$$

Our model a will account for the effect of target inelastic channels on the elastic channel. This effect, as mentioned earlier for the case of Ps-H scattering [23,25], is of key importance in determining the low-energy elastic parameters. In our model b, in addition to the target excitation (up to $n = 2$ singlet state), we have taken the $2p$ excitation of the Ps atom. Our experience on Ps-H and Ps-He scattering show that inclusion of the Ps $2s$ -state affects the low-energy elastic scattering parameters marginally. Model b also includes excitation of both the atoms simultaneously to $2p$ state. This inclusion partially allows us to include the lowest-order long-range force, i.e., van der Waals' interaction, dynamically. In the next section, we briefly describe the theoretical part of our calculation to make the article self-consistent.

THEORY

The total wave function for the system comprised of a positronium atom and a helium atom should be antisymmetric and may be expressed as,

$$\Psi^\pm(\vec{r}_p, \vec{r}_1, \vec{r}_2, \vec{r}_3) = (1 \pm P_{12}) \sum_{n\nu} \eta_\nu(\rho_1) \Phi_n(\vec{r}_2, \vec{r}_3) F_{n\nu}^+(\vec{R}_1), \quad (1)$$

where, $\vec{R}_i = \frac{1}{2}(\vec{r}_p + \vec{r}_i)$ and $\vec{\rho}_i = (\vec{r}_p - \vec{r}_i)$; $i = 1, 2$.

Here, η_ν and Φ_n are the eigenfunctions of the positronium atom and helium atom, respectively. \vec{r}_i and \vec{r}_p are the position vectors of the electrons and that of positron, respectively. All the distances are measured from the center of mass of the system, which effectively lies with the nucleus of the He atom. P_{12} is the exchange operator.

The total Hamiltonian for the system is given by,

$$H = -\frac{1}{4}\vec{\nabla}_{R_1}^2 + H_{\text{Ps}}(\vec{p}_1) + H_{\text{He}}(\vec{r}_2, \vec{r}_3) + V_{\text{int}}(\vec{r}_p, \vec{r}_1, \vec{r}_2, \vec{r}_3), \quad (2)$$

where V_{int} is the interaction potential and is given by

$$V_{\text{int}}(\vec{r}_p, \vec{r}_1, \vec{r}_2, \vec{r}_3) = \frac{2}{r_p} - \frac{2}{r_2} - \frac{1}{|\vec{r}_p - \vec{r}_1|} + \frac{1}{|\vec{r}_1 - \vec{r}_2|} - \frac{1}{|\vec{r}_p - \vec{r}_3|} + \frac{1}{|\vec{r}_2 - \vec{r}_3|}, \quad (3)$$

Here, H_{Ps} and H_{He} are the Hamiltonians describing the bound Ps and He atoms, respectively, and they satisfy the following Schrödinger equations,

$$H_{\text{Ps}}\eta_\nu = \varepsilon_\nu\eta_\nu,$$

$$H_{\text{He}}\Phi_n = \varepsilon_n\Phi_n.$$

The three-dimensional coupled integral equation, in the momentum space, for the scattering amplitude, may be expressed as

$$\begin{aligned} \langle K'n'\nu' | Y^\pm | Kn\nu \rangle &= \langle K'n'\nu' | B^\pm | Kn\nu \rangle + \sum_{n''} \sum_{\nu''} \int d\vec{k}'' \\ &\times \frac{\langle K'n'\nu' | B^\pm | K''n''\nu'' \rangle \langle K''n''\nu'' | Y^\pm | Kn\nu \rangle}{E - E'' + i\varepsilon} \end{aligned} \quad (4)$$

where

$$\begin{aligned} \langle K'n'\nu' | Y^\pm | Kn\nu \rangle &= \langle K'n'\nu' | Y_{11} | Kn\nu \rangle \\ &\pm \langle K'n'\nu' | Y_{21} | Kn\nu \rangle. \end{aligned}$$

Here, the transition matrix element of Y_{11} stands for the direct channel and the matrix element Y_{21} is that for the exchange channel. A similar expression for the matrix element B^\pm holds good. The transition matrix elements of B_{11} and B_{21} give the first Born and Born-Oppenheimer amplitudes, respectively. Calculation of direct (FBA) are straight forward. The exchange scattering amplitude in the plane-wave approximation, for elastic as well as the $n=2$ Ps excitation, where the He atom is in the ground state, has been evaluated by Sarkar, Chaudhuri, and Ghosh [10]. Here, we provide the final expression for the projectile-elastic scattering amplitudes up to $n=2$ singlet excitation of the He atom in the Appendix.

In the atom-atom system both the atoms have internal degrees of freedom, unlike e^- (e^+)-atom scattering. Therefore, each channel has three angular momenta and the angular momentum has to be conserved due to rotational symmetry. Hence, one does require to employ a coupled-state representation for the three angular momenta for each channel. Keeping this in mind, scattering amplitude may be expanded as [25,27]

$$\begin{aligned} f_{\eta' \nu'; \eta \nu}^+(\vec{k}', \vec{k}) &= \frac{1}{\sqrt{k k'}} \sum_{JM J_1 M_1 J'_1 M'_1 L M_L L' M'_L} \begin{pmatrix} L' & l'_p & J'_1 \\ M'_L & m'_p & M'_1 \end{pmatrix} \\ &\times \begin{pmatrix} J'_1 & l'_a & J \\ M'_1 & m'_a & M \end{pmatrix} Y_{L' M'_L}^*(\hat{k}') T^{J^\pm}(\tau' k'; \tau k) Y_{L M_L}(\hat{k}) \\ &\times \begin{pmatrix} L & l_p & J_1 \\ M_L & m_p & M_1 \end{pmatrix} \begin{pmatrix} J_1 & l_a & J \\ M_1 & m_a & M \end{pmatrix}. \end{aligned} \quad (5)$$

Here, l_a and l_p are the orbital angular momenta of the bound target and the projectile atoms, respectively, with projections m_a and m_p . L is the angular momentum of the moving Ps atom with projection M_L . L combines with l_p to yield J_1 , which again couples with l_a to give the good quantum number J with projection M . All these quantities are referred to the initial channel. The corresponding final channel components are denoted by primes. Note that $f_{\eta' \nu'; \eta \nu}^{B^\pm}(\vec{k}', \vec{k})$ have similar expressions with $T^{J^\pm}(\tau' k'; \tau k)$ replaced by $B^{J^\pm}(\tau' k'; \tau k)$.

After the partial-wave analysis, we obtain one-dimensional coupled integral equation for T^{J^\pm} :

$$\begin{aligned} T^{J^\pm}(\tau' k'; \tau k) &= B^{J^\pm}(\tau' k'; \tau k) - \frac{1}{2\pi^2} \\ &\times \sum_{\tau''} \int \frac{B^{J^\pm}(\tau' k'; \tau'' k'') T^{J^\pm}(\tau'' k''; \tau k)}{k_{\eta' \nu''}^2 - k''^2 + i\varepsilon} \\ &\times k'' dk'', \end{aligned} \quad (6)$$

where $\tau \equiv (n_p, l_p, n_a, l_a, L, J)$. Equation (6) is solved by the matrix inversion technique for each partial wave using our own numerical code.

The partial wave added CCA cross section in units of πa_0^2 for the transition $\text{Ps}(1s) + \text{He}(1s^2) \rightarrow \text{Ps}(n_p, l_p, m_p) + \text{He}(1s; n_a^1, l_a, m_a)$ is given by the relation,

$$\sigma_J^{\text{CCA}} = \sum_{JJ_1^*, L'} \frac{2J+1}{4\pi^2 k^2} |T^J(\tau k; \tau_0 k)|^2. \quad (7)$$

The elastic phase shift for the J th partial wave is given by

$$\delta_J(k) = \frac{1}{2} \tan^{-1} \left\{ \frac{\text{Re}[T^J(\tau_0 k; \tau_0 k)]}{2\pi - \text{Im}[T^J(\tau_0 k; \tau_0 k)]} \right\}, \quad (8)$$

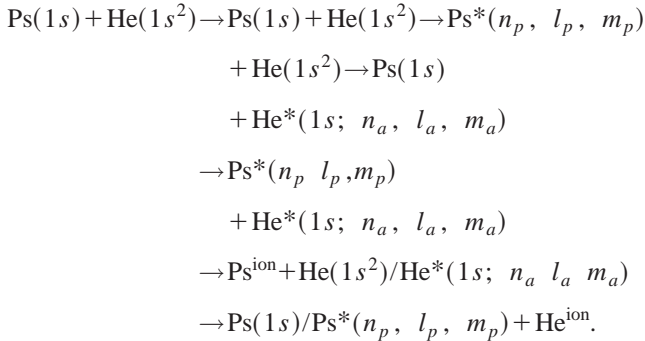
where, the ground state of Ps-He is represented as $\tau_0 \equiv (1, 0, 1, 0; J, J)$.

The partial-wave Born cross section is given by a similar relation as in Eq. (7),

$$\sigma_J^B = \sum_{JJ_1^*, L'} \frac{2J+1}{4\pi^2 k^2} |B^J(\tau k; \tau_0 k)|^2. \quad (9)$$

The total cross section is the sum of all partial cross sections when they are energetically accessible. To compare our

predictions with the measured data, we do require to calculate the higher excitations and ionization of the Ps atom, excitations and ionization of the He atom, and excitations of both the atoms simultaneously. We have picked up the following processes to predict the total cross section:



The superscript * indicates the discrete excitation of the atom concerned. Here, we neglected the effect of continuum of both the atoms.

We have calculated the elastic cross section as well as low-lying excitation cross sections and also up to $n=2$ excitations of both the atoms using our CCA model. In calculating the ionization cross sections above the ionization threshold, we have neglected the electron exchange between the atoms. The higher excitation of the projectile and target atom is calculated by the first Born-Oppenheimer (B-O) approximation. Double excitation has also been calculated by B-O approximation for higher excited states.

Expression of the scattering amplitude for the Ps ionization combined with arbitrary excitation of the He atom is given by

$$\begin{aligned}
f_{\text{Ps}}^{\text{B(ion)}} = \frac{4}{Q^2} \langle \eta(c) | e^{i\vec{Q}\cdot\vec{\rho}_1/2} - e^{i\vec{Q}\cdot\vec{\rho}_1/2} | \eta_{1s}(\vec{\rho}_1) \rangle \times \langle \Phi_{1s^2}(\vec{r}_2, \vec{r}_3) | 2 \\
- e^{i\vec{Q}\cdot\vec{r}_2} - e^{i\vec{Q}\cdot\vec{r}_3} | \Phi_{1s^2}(\vec{r}_2, \vec{r}_3) \rangle, \quad (10)
\end{aligned}$$

where \vec{Q} is the momentum transfer. $\eta(c)$ is the continuum wave function for the Ps atom.

In calculating the He ionization, in which the exchange of electrons has been neglected, we consider a transition of the Ps atom to a p state in order to make the integral nonvanishing. Our final state is comprised of a symmetrized wave function for the He atom given by

$$\Phi_f = \frac{1}{\sqrt{2}} [u^\dagger(\vec{r}_3) \phi_{K_c}(z, \vec{r}_2) + u^+(\vec{r}_2) \phi_{K_c}(z, \vec{r}_3)], \quad (11)$$

where $u^+(r) = (\lambda^{3/2}/\sqrt{\pi}) e^{-\lambda x}$; $\lambda=2$ and $\phi_{K_c}(z, \vec{r}) = \chi_{K_c}(z, \vec{r}) - \langle \chi_{K_c}(z, \vec{r}') | \Phi_0(\vec{r}') \rangle \Phi_0(\vec{r})$.

Here, $\chi_{K_c}(z, \vec{r})$ is the continuum wave function for the ejected electron in the attractive Coulomb field of nucleus with nuclear charge $Z=1$.

Expression of the scattering amplitude for the He ionization combined with the Ps excitation to p -states is given by

$$\begin{aligned}
f_{\text{He}}^{\text{B(ion)}} = \frac{4}{Q^2} \langle \eta_{np}(\vec{\rho}_1) | e^{i\vec{Q}\cdot\vec{\rho}_1/2} - e^{-i\vec{Q}\cdot\vec{\rho}_1/2} | \eta(\vec{\rho}_1) \rangle \\
\times \langle \Phi_f | 2 - e^{i\vec{Q}\cdot\vec{r}_2} - e^{i\vec{Q}\cdot\vec{r}_3} | \Phi_{1s^2}(\vec{r}_2, \vec{r}_3) \rangle \quad (12)
\end{aligned}$$

Now, the total cross section for Ps-He scattering is given by the relation,

$$\begin{aligned}
\sigma^T = \sigma_{\text{el}}^{\text{CCA}} + \sigma_{\text{Ps}(n=2)}^{\text{CCA}} + \sigma_{\text{He}(n=2)}^{\text{CCA}} + \sigma_{\text{Ps}(2<n\leq 4)}^{\text{B-O}} + \sigma_{\text{He}(2<n\leq 4)}^{\text{B-O}} \\
+ \sigma_{\text{ion(Ps)}}^{\text{BG}} = \sigma_{\text{ion(He)}}^{\text{FBA}} \quad (13)
\end{aligned}$$

where, $\sigma_{\text{el}}^{\text{CCA}}$ is the elastic cross section using model (b); $\sigma_{\text{Ps}(n=2)}^{\text{CCA}}$ is the Ps($n=2$) excitation cross sections; $\sigma_{\text{He}(n=2)}^{\text{CCA}}$ is the He($n=2$) excitation (singlet) cross sections; $\sigma_{\text{Ps}(2<n\leq 4)}^{\text{B-O}}$ is the Ps excitation ($n=3$ and 4) cross section and $\sigma_{\text{He}(2<n\leq 4)}^{\text{B-O}}$ is the He ($n=3$ and 4) excitation cross section using first-order Born-Oppenheimer approximation; $\sigma_{\text{ion(Ps)}}^{\text{BG}}$ is the Ps ionization cross section as given by Belfast group [11], and $\sigma_{\text{ion(He)}}^{\text{FBA}}$ is the He ionization contribution. Except for the $\sigma_{\text{el}}^{\text{CCA}}$, the other partial cross sections are added to the total cross section when they are energetically accessible.

RESULTS AND DISCUSSIONS

We have solved the one-dimensional coupled integral equation (6) by matrix inversion method using our own numerical code. In solving the integral equation we have to obtain the partial wave Born amplitude for each process. To evaluate Born amplitudes we use singlet wave function of the He atom given by Winter and Lin [28]. As a check of our program, angle integrated Born cross sections using nonpartial wave and partial wave methods have been tested. Convergence of the integral equation has also been verified by changing the number of integration points between $0-2k$ and $2k-\infty$. We reproduced the results of Sarkar and Ghosh [9] from this combined code.

We calculate the CCA cross section for $J=N$ (suppose). We choose the value of N such that the partial wave CCA cross section for $J=N$ is very close to the corresponding partial wave Born cross section. The higher partial cross section is replaced by the corresponding Born cross section. Analytically, it may be expressed as,

$$\sigma^{\text{CCA}} = \sigma_{J(=N)}^{\text{CCA}} + \sigma^{\text{B}} - \sigma_{J(=N)}^{\text{B}}. \quad (14)$$

At the lowest energy (i.e., 0.068 eV), we have calculated the partial wave CCA cross section up to $N=3$, while at the highest energy (i.e., 110 eV) corresponding value is $N=12$. We would like to add that, below the first excitation threshold of the system, convergent results have been obtained with $N=3$. Both the CCA and Born partial wave cross section nearly vanish beyond this partial wave.

We start to present our results with the low-lying phase shifts. This is because phase shift is a sensitive test for the methodology employed. In Table I, we quote S -wave phase

TABLE I. S -wave phase shifts, in units of radians and scattering length, a_0 , using different models.

K (a.u.)	Static exchange		3 ST TE CCA		Model a	Model b
	Sarkar and Ghosh [9]	Sarkar, Chaudhuri, and Ghosh [10]	Model a	Model b		
0.1	2.951		2.9514		3.00	3.01
0.2	2.763		2.764		2.86	2.87
0.3	2.582		2.584		2.72	2.73
0.4	2.410		2.412		2.58	2.59
0.5	2.248		2.260		2.44	2.45
0.6	2.100		2.103		2.31	2.32
0.7	1.961		1.966		2.18	2.19
0.8	1.836		1.843		2.06	2.07
	Drachman and Houston		Model a		Model b	
Scattering length	1.389		1.394		1.360	

shifts using our present two models along with the static exchange results of Sarkar and Ghosh [9] and three-state target elastic results of Sarkar, Chaudhuri, and Ghosh [10]. Table I also contains the value of scattering length and compares those with the result of Drachman and Houston [7]. For visual display, Fig. 1 represents S -wave phase shifts of Ps-He scattering as tabulated in Table I. The static exchange and three-state target elastic results differs marginally from each other. A similar feature has also been obtained by the present two models. Difference between the results of model a and model b is below 0.5%. The present S -wave phase shifts clearly indicate that it is the effect of the target excitation that influences the scattering parameters dominantly below the first excitation threshold and not the projectile excitation. Moreover, van der Waals' interaction that has been included dynamically in model b is also not found to be significant at these energies, at least for the case of Ps-He scattering. It is

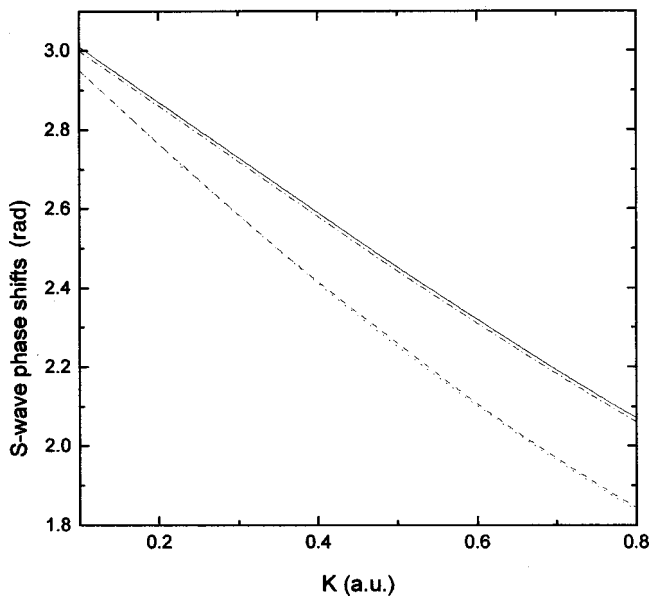


FIG. 1. S -wave phase shifts. Curves: dot, static exchange; dash, three-state target elastic CCA; dash-dot, model a; solid, model b.

very interesting to note that S -wave phase shifts obtained by our present model, that includes the target inelastic channels, differ significantly from those of Sarkar, Chaudhuri, and Ghosh [10]. Present S -wave phase shifts necessarily indicate that the effect of target excitation on the elastic-scattering parameters is appreciable when compared with those of projectile excitation. Scattering length obtained using model a is very close to that predicted by Drachman and Houston [7]; the value of model a being higher. But, scattering length, predicted by our model b, is slightly lower than the predictions of model a as well as that of Drachman and Houston. The present results using model b are expected to be more accurate than those of model a as model b is theoretically more sound than model a and is also expected to be more reliable than those of Drachman and Houston. It is evident due to the fact that they have included the effect of exchange via the local model exchange potential. However, findings of Blackwood *et al.* [11] indicate that inclusion of higher excited states and continuum of the projectile atom may further reduce the present scattering length, although not appreciable.

There is an anomaly in the theoretical predictions as well as measured data for total cross section at zero or near zero energy. We will come to this point later.

Our P -wave phase shifts using both the present models are plotted in Fig. 2. Figure 2 also presents static exchange results of Sarkar and Ghosh [9] and three-state target elastic of Sarkar, Chaudhuri, and Ghosh [10]. Static exchange and three-state target elastic results are very close to each other as has also been seen in the S -wave phase shifts. Our present model b predicts the highest value whereas static exchange predicts the lowest one. Our model b results differ appreciably from the results of Sarkar, Chaudhuri, and Ghosh [10] as well as model a. Difference between the results of model a and model b increases with energy below the first excitation threshold. S - and P - wave phase shifts reported here using models a and b are found to be variationally consistent. This is due to the fact that with the addition of higher excited states the phase shifts increase, which is a variationally consistent phenomenon.

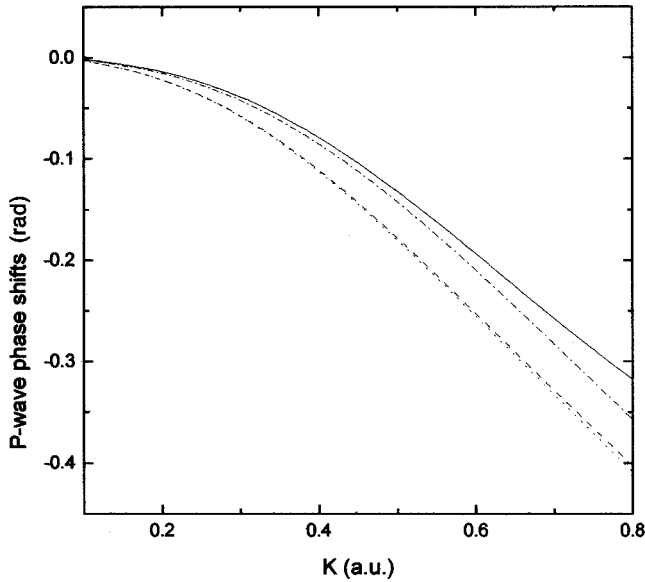


FIG. 2. P -wave phase shifts. Curves: dot, static exchange; dash, three-state target elastic CCA; dash-dot, model a; solid, model b.

Our D -wave phase shifts using both the present models along with static exchange and three-state target elastic results are plotted in Fig. 3. The qualitative feature of S - and P -wave phase shifts is also present in the D -wave results. Static exchange and three-state target elastic results are close to each other, while model a and b results differ marginally. Model b predicts the highest values; static exchange results are the lowest. As in the case of the S - and P -wave, the D -wave phase shifts are variationally consistent.

Figure 4 depicts the elastic cross sections of present models and they are compared with most elaborate target elastic results of the Belfast group [11] and those of static exchange [9]. The Belfast group predicts the results up to the incident positronium energy 40 eV. Static exchange result, at zero

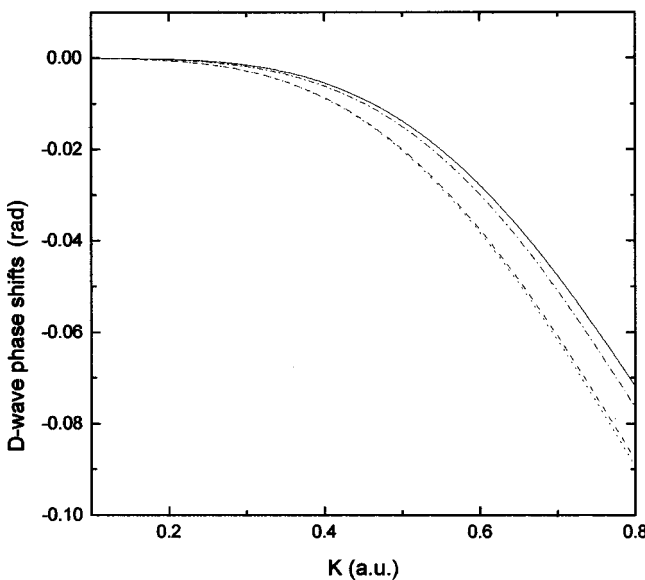


FIG. 3. D -wave phase shifts. Curves: dot, static exchange; dash, three-state target elastic CCA; dash-dot, model a; solid, model b.

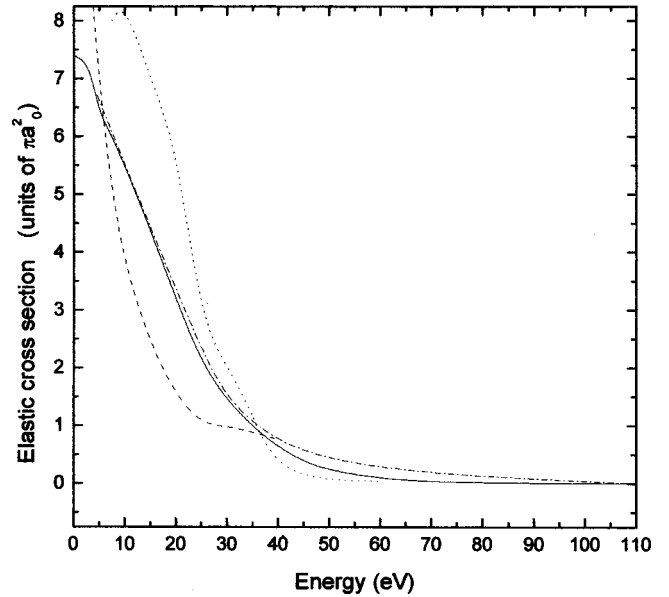


FIG. 4. Elastic cross section. Curves: dot, static exchange; dash, Blackwood *et al.* [11]; dash-dot, model a; solid, model b.

energy, is $14.584\pi a_0^2$ and that predicted by the Belfast group is $13.193\pi a_0^2$. The results using present models, dramatically differ from those of the Belfast group [11] as well as Sarkar and Ghosh [9] and Sarkar, Chaudhuri, and Ghosh [10] (not shown). The elastic cross section, which is the total cross section at zero energy, is $7.78\pi a_0^2$ using model a and $7.4\pi a_0^2$ using model b. The result of the Belfast group nearly coincides with that of projectile elastic prediction of model a at 40 eV, whereas, static exchange results coalesce with that of model b above 60 eV. Slope of the elastic cross section obtained by the Belfast group [11] and Sarkar and Ghosh [9] is more steep than the corresponding slopes of model a and b. These suggest that the effect of projectile inelastic channels influence the elastic cross section appreciably beyond the first excitation threshold, i.e., 5.1 eV. At the incident Ps energy of 110 eV, all the sets of the result are almost identical. As a future reference, we have given the values of elastic results of model a and b in Table II.

Total cross section of Ps-He scattering in the incident energy range 0–110 eV is shown in Fig. 5. Our total cross section using model (b) is depicted here. The present total cross section is calculated by relation (13). In Fig. 6, we display three partial cross sections so as to make Fig. 5 self-explanatory as well as to avoid complicity and overcrowding of curves in the figure. The theoretical prediction for total cross section by Sarkar, Chaudhuri, and Ghosh [10], Blackwood *et al.* [11], Peach [26], and Biswas and Adhikari [12] are given for comparison. Experimental data of the UCL group in the energy region 10–110 eV and zero or near zero energy predictions of Nagashima *et al.* [19], Canter, McNutt, and Roellig [20], Coleman *et al.* [21], and Skalsey *et al.* [22] are shown in the figure. Theoretical predictions of Drachman and Houston [7] at zero energy is also shown in the same figure.

Let us now start the discussion of zero or near zero energy cross section. Total cross section up to 5.1 eV is just the

TABLE II. Elastic cross sections using model (a) and model (b), in units of πa_0^2 .

Energy in eV	Model a	Model b
0.0	7.78	7.40
2.5	7.40	7.30
4.0	7.21	7.10
5.0	6.89	6.47
6.0	6.67	6.25
7.5	6.32	6.00
10.0	5.74	5.50
15.0	4.55	4.40
20.0	3.48	3.20
25.0	2.39	2.09
30.0	1.56	1.44
35.0	1.08	9.82(-1)
40.0	7.70(-1)	6.43(-1)
45.0	5.72(-1)	3.81(-1)
50.0	4.52(-1)	2.28(-1)
60.0	2.94(-1)	8.69(-2)
75.0	1.66(-1)	2.22(-2)
90.0	8.52(-2)	5.86(-3)
110.0	1.34(-2)	1.31(-3)

elastic cross section. Measured data of different groups using time-of-flight technique, do not tally among themselves. Measured data at zero or near zero energies vary between 2.6 to $13\pi a_0^2$. Similarly, theoretical predictions run from 2.7 to $14.5\pi a_0^2$. Nagashima *et al.* [19] have obtained, at zero en-

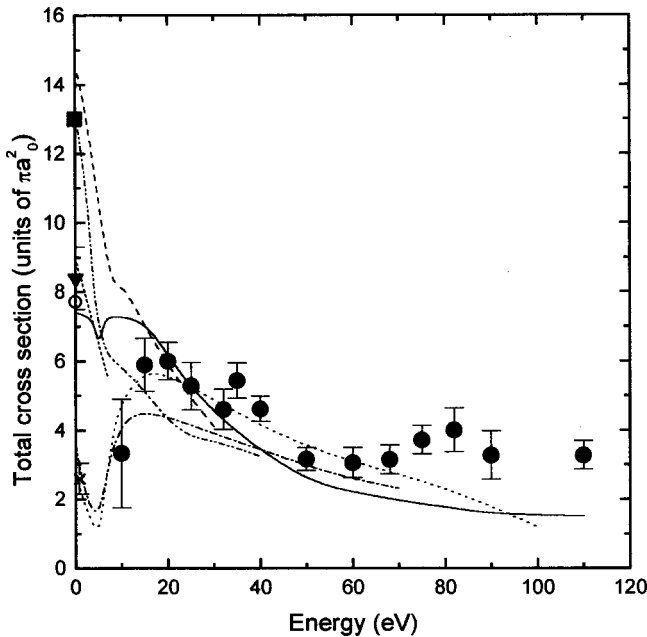


FIG. 5. Total cross section. Curves: dot, Biswas and Adhikari [12]; dash, Sarkar *et al.* [11]; dash dot, Peach [26]; dash-double dot, Blackwood *et al.* [11]; short dash, Coleman *et al.* [21]; solid, model b; solid circle, UCI group [18]; solid square, Nagashima *et al.* [19]; solid inverted triangle, Canter *et al.* [20]; cross, Skalsey *et al.* [22]; hollow circle, Drachman and Houston [7].

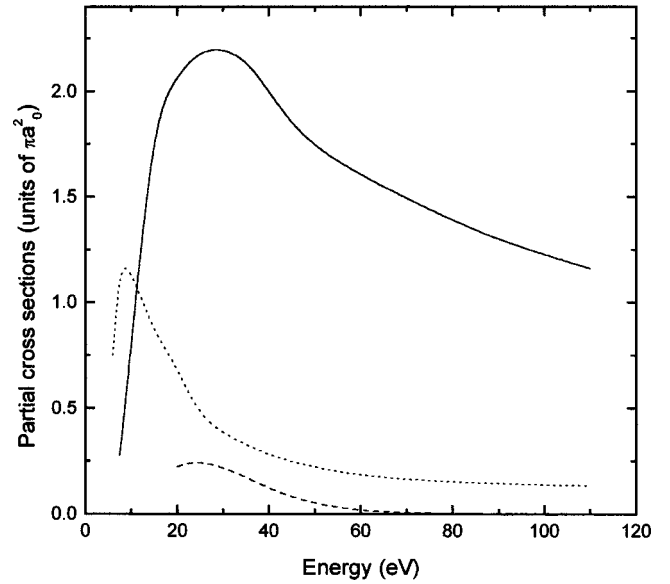


FIG. 6. Partial cross sections. Curves: dot, Ps excitation; dash, He excitation; solid, Ps ionization.

ergy, $13(\pm 4)\pi a_0^2$, which is very close to the prediction of Sarkar, Chaudhuri, and Ghosh [10] ($14.584\pi a_0^2$) and Blackwood *et al.* [11] ($13.193\pi a_0^2$). On the other hand, measured data of Skalsey *et al.* $2.6(\pm 0.5)\pi a_0^2$ is close to the theoretical predictions of Peach [26] ($3.3\pi a_0^2$) and Biswas and Adhikari [12] ($2.7\pi a_0^2$). Skalsey *et al.* [22] has used the time-resolved Doppler broadening spectroscopy to estimate the cross section. Our present results of model a and b, shown in Fig. 4, are $7.78\pi a_0^2$ and $7.4\pi a_0^2$, respectively. The theoretical prediction of Drachman and Houston is $7.73\pi a_0^2$, which is in very good agreement with the present results. These values are also very close to measured data of Canter *et al.* [20] ($8.4 \pm 0.9\pi a_0^2$). Total cross section of Coleman *et al.* [21], without error bar, is $9 - 0.5E\pi a_0^2$, where E is the incident energy. Three-state projectile elastic results of Sarkar, Chaudhuri, and Ghosh [10] is not very much different from the 22-state target elastic pseudostate results of Blackwood *et al.* [11]. Thus, it is apparent that the loss of inelastic flux of the Ps atom will not affect the zero energy cross section significantly. It has been found by us that the effect of target inelastic channels is of key importance in determining zero or near zero energy cross section [23–25,29]. This has been supported by the work of Peach [26] who has taken the effect of target inelastic channels through an adiabatic model potential. Drachman and Houston [7], although they used a model local exchange potential, have taken the effect of target excitation through their eighty-four term close channel wave function. It may be mentioned that the adiabatic effect is expected to be valid at the asymptotic region, whereas for small separation the nonadiabatic effect plays its part. This may be the reason for low value of cross section at zero energy as given by Peach [26]. Biswas and Adhikari [12] has also predicted a low value very close to that of Skalsey *et al.* [22]. They have used a model nonlocal exchange potential in the calculations. Therefore, it is very difficult to assess the accuracy of their results. Biswas and

Adhikari [12] has argued about the nonorthogonality of the exchange channel wave function. We feel this is not that serious as pointed out by them. In this connection, we refer to e^- -atom scattering calculations. In our investigation, we have neglected the effect of continuum of both the atoms. By far the most elaborate target elastic calculation, including the effect of continuum of Ps through pseudostates, Blackwood *et al.* [11], have shown explicitly that zero energy cross section is not going to change significantly. We have calculated the ionization of the He atom by positronium impact using the Coulomb Born approximation. It has been found that the He ionization gives a peak at about 35 eV and its value is of the order of 10^{-3} in units of πa_0^2 . Hence it is not unwise to assume that effect of target continuum may influence the elastic cross section marginally. Here in the expansion scheme, we have not included the eigenstates beyond $n=2$ for both the atoms. Therefore, inclusion of higher excited states in the basis set may modify the results slightly near zero energy. Therefore, zero energy cross section is expected to lie in the vicinity of the present results.

We define total cross section as given by the relation (13). The present total cross section thus defined is plotted in Fig. 5. There is a minimum in the present results near the first excitation threshold. This feature has also been noticed by Peach [26] and Biswas and Adhikari [12]. However, the values of cross section of Peach [26] and Biswas and Adhikari [12] are very much different from that of ours. This feature has also been noticed by us in our earlier communication [29]. On the other hand, Sarkar, Chaudhuri, and Ghosh [10] and Blackwood *et al.* [11] do not show such well-defined minimum. However, there is a change of slope in their predications slightly above this energy. The higher ($n>2$) partial cross sections for Ps excitation have been added to the total cross section by Blackwood *et al.* [11], which is not shown in their Table I [30]. The elastic cross section decreases with increase in energy while, above 5.1 eV the inelastic channels of the Ps atom become energetically accessible and the Ps excitation cross sections are added to the elastic cross section. This in turn raises the total cross section. Hence, the minimum in total cross section is well expected. Present results are in qualitative agreement with the measured data of the UCL group above 15 eV. Present results are in excellent agreement in the energy range 20–30 eV, while beyond this energy range the predictions lie below the measured data. It may be mentioned that present results fail to reproduce the humps measured by the UCL group in the energy range 30–40 eV and 75–85 eV. All the theoretical models have the same feature. Results of Blackwood *et al.* [11], up to the incident energy 40 eV, are at variance with those of ours. The results of Sarkar, Chaudhuri, and Ghosh [10] are not very much different from those of the present in the energy range 15–30 eV. Results of Peach [26] and Biswas and Adhikari [12], up to the incident energy 10 eV, are in fair agreement among themselves as well as are in good agreement with the measured data. In this energy range these results are very much different from other theoretical predictions. The best agreement between theory and experiment is given by Biswas and Adhikari [12] using

their phenomenological model. However, above 70 eV their data deviates appreciably from the measured data.

The ionization cross section of Ps atom plays a crucial role in predicting the total cross section when it is energetically accessible. The ionization of the Ps atom is the most dominant contributor to the total cross section beyond 50 eV. The elastic cross section is very small beyond 50 eV. Elastic and other excitation cross sections are negligible compared to the ionization of the Ps atom at about 100 eV. Therefore, to predict a reliable total cross section, the ionization cross section has to be evaluated with proper care. Good agreement between the predictions of Biswas and Adhikari [12] and measured data of the UCL group up to incident energy 70 eV is due to the fact that their ionization cross section, using their nonlocal exchange potential, is about twofold that of Blackwood *et al.* [11]. However, Biswas and Adhikari [12] did not calculate the ionization cross section using Born-Oppenheimer approximation by antisymmetrizing the total wave function. The validity of the results has not been tested. Blackwood *et al.* [11], in their model, have included the pseudostates to evaluate ionization cross section. Their results are expected to be more reliable than the first Born results. Hence, we have included the ionization of Blackwood *et al.* [11] in defining our total cross sections. We have extrapolated the results of Blackwood *et al.* [11] up to 110 eV, so that we can present our results up to the quoted range. More exact evaluation of ionization cross section may modify the results to some extent.

CONCLUSION

We investigate the scattering of Ps atoms off He target in the incident energy range 0–110 eV. We have employed close-coupling approximation using two basis sets. In the first basis set, we allow the excitation of target He atom up to the $n=2$ singlet state and restricted the projectile atom to its ground state. In our second expansion scheme, we have allowed internal degrees of freedom of both the atoms and retained up to $n=2$ eigenstates for each atom. At medium energies, measured data are due to the UCL group. However, at zero or near zero energies, four experimental data are available for comparison, using time-of-flight measurements [19–21] and Doppler broadening spectroscopy [22]. All the experimental data are at variance widely among themselves. There is no prior reason to prefer one experimental value over the other. On the other hand, theoretical estimates at zero or near zero energies differ among themselves, similar to the case of measured values. However, one can judge the validity and accuracy of the theoretical models employed to calculate zero energy cross section. Sarkar, Chaudhuri, and Ghosh [10] and Blackwood *et al.* [11] have restricted the internal degrees of freedom of the target atom. It is worth mentioning that model of Blackwood *et al.* [11] in the framework of target elastic close-coupling approximation is the most accurate one. Drachman and Houston [7] have used a model local exchange potential and solved the equations using a close channel wave function having eighty-four terms. Their close channel wave function has taken into account the internal degrees of freedom of both the atoms and their cor-

relation effect. Error included in their model is mainly due to the local exchange potential. Proper inclusion of Pauli exclusion principle will modify their results. It has also been pointed in the text that Peach has included the effect of target excitation adiabatically. This adiabatic model may vitiate the results at zero energy. As already pointed out earlier, it is very hard to estimate the accuracy of the results of Biswas and Adhikari. Literature reveals that the effect of virtual excitation and ionization of Ps atoms are not the only determining factors for the elastic cross section at zero energy. The present models, as well as work of Drachman and Houston and Peach, show that the effect of inelastic channels of the target atom is most significant. Our model b includes excitation of both the atoms explicitly and the van der Waals' interaction is partially accounted for dynamically. Hence, model b can be considered as the most realistic model so far carried out to investigate Ps-atom scattering. More elaborate calculation using this model may modify the results but our wisdom tells us that modified results will not be very different from the results predicted by the present model.

It has been found that elastic cross section obtained by different models converges at about 100 eV. Predictions of Blackwood *et al.* suggest that in the intermediate energy range (5–40 eV) the effect of virtual excitation of Ps atoms may influence the cross sections. In calculating the ionization cross section, the exchange effect has not been taken into consideration. The higher excitation cross sections, estimated by the first-order theory, may also be calculated using a more realistic model. Calculation of the exact value of the Ps ionization and more reliable partial cross sections, other than elastic one and $n=2$ excitation ones, is expected to modify the total cross section at medium and high energies, although not expected to be significant. All the theoretical predictions at medium and high energies differ from the measured data of the UCL group. This necessarily warrants further experimental studies for these processes.

We advocate for a calculation with a larger basis set allowing internal degree of freedom for both the atoms and also the partial cross sections of the higher excited states for both the atoms and especially the ionization of the Ps atom should be evaluated using a more theoretically sound model.

ACKNOWLEDGMENTS

The authors are thankful to Department of Science and Technology, Government of India for the financial support (SP/S2/K-31/96). One of us, A.B. is grateful to CSIR, Government of India for his financial support (F. No. 9/80(297)/99-EMR-I).

APPENDIX

In the calculation of the o -Ps-He exchange scattering amplitude we have considered 2^1s and 2^1p states of the He atom. Calculation of 2^1s matrix element is comparatively easier than 2^1p . Here, we are only giving the exchange Born scattering amplitude for the process $\text{Ps}(1s) + \text{He}(1s^2) \rightarrow \text{Ps}(1s) + \text{He}(1s2^1p)$. The required exchange Born matrix element is

$$f^{\text{B-O}}(\vec{k}, \vec{k}') = -\frac{\mu}{2\pi} \int \exp -i\frac{1}{2}\vec{k}' \cdot (\vec{r}_p + \vec{r}_2) \\ \times \eta_{1s}(|\vec{r}_p - \vec{r}_2|) \Phi_{n^1l}^*(\vec{r}_1, \vec{r}_3) \\ \times (H-E) \exp i\frac{1}{2}\vec{k} \cdot (\vec{r}_p + \vec{r}_1) \\ \times \eta_{1s}(|\vec{r}_p - \vec{r}_1|) \Phi_{1s^2}(\vec{r}_2, \vec{r}_3) d\vec{r}_p d\vec{r}_1 d\vec{r}_2 d\vec{r}_3. \quad (\text{A1})$$

$(H-E)$ operates on the final state total wave function and takes the form (off the energy shell),

$$(E'' - E) + V_{\text{int}}(\vec{r}_p, \vec{r}_1, \vec{r}_2, \vec{r}_3),$$

where $V_{\text{int}}(\vec{r}_p, \vec{r}_1, \vec{r}_2, \vec{r}_3)$ is given by Eq. (3).

Now the wave functions may be expressed as

$$\eta_{1s}(\rho) = \frac{1}{\sqrt{8\pi}} e^{-\alpha_i \rho}; \quad \alpha_i = 0.5,$$

$$\Phi_{1s^2}(\vec{r}, \vec{r}') = u_{1s}(\vec{r}) u_{1s}(\vec{r}'),$$

$$u_{1s}(\vec{r}) = N(1s) \sum_{m=1}^2 a_m(1s) e^{-\beta_m^r},$$

$$\Phi_{1s2^1p}(\vec{r}, \vec{r}') = \frac{1}{\sqrt{2}} N(2p) \{u^+(\vec{r}) v_{2p}(\vec{r}') + u^+(\vec{r}') v_{2p}(\vec{r})\}$$

$$u^+(\vec{r}) = \left(\frac{8}{\pi}\right)^{1/2} e^{-Z_n r}; \quad Z_n = 2.0,$$

$$v_{2p}(\vec{r}) = b(2p) r Y_{1m}(\hat{r}) e^{-\delta r}.$$

The parameters of the target wave function are given in Ref. [28].

After performing the integration over $d\vec{r}_3$, the scattering amplitude reduces to the form,

$$f^{\text{B-O}}(\vec{k}, \vec{k}') = -\frac{\mu}{2\pi} \frac{1}{\sqrt{2}} N(2p) [I_1 + I_2 + I_3 + I_4], \quad (\text{A2})$$

where, μ is the reduced mass of the system and is equal to 2.

$$I_1 = (E'' - E) A \int C(\vec{r}_p, \vec{r}_1, \vec{r}_2) d\vec{r}_p d\vec{r}_1 d\vec{r}_2, \quad (\text{A3})$$

$$I_2 = A \int C(\vec{r}_p, \vec{r}_1, \vec{r}_2) \left\{ \frac{1}{r_p} - \frac{1}{r_2} - \frac{1}{|\vec{r}_p - \vec{r}_1|} \right. \\ \left. + \frac{1}{|\vec{r}_1 - \vec{r}_2|} \right\} d\vec{r}_p d\vec{r}_1 d\vec{r}_2, \quad (\text{A4})$$

$$I_3 = 16\sqrt{2}\pi N(1s) \sum_m a_m(1s) \frac{1}{\lambda_m^3} \times \int \left\{ \frac{e^{-\lambda_m r_p}}{r_p} - \frac{e^{-\lambda_m r_2}}{r_2} + \frac{\lambda_m}{2} (e^{-\lambda_m r_p} - e^{-\lambda_m r_2}) \right\} C(\vec{r}_p, \vec{r}_1, \vec{r}_2) d\vec{r}_p d\vec{r}_1 d\vec{r}_2, \quad (\text{A5})$$

$$C \equiv \eta_{1s}(|\vec{r}_p - \vec{r}_2|) \eta_{1s}(|\vec{r}_p - \vec{r}_1|) \exp i \frac{1}{2} \vec{Q} \cdot \vec{r}_p \times \exp \left(-i \frac{1}{2} \vec{k}' \cdot \vec{r}_2 \right) \exp \left(i \frac{1}{2} \vec{k} \cdot \vec{r}_1 \right) v_{2p}(\vec{r}_1) u_{1s}(\vec{r}_2), \quad (\text{A9})$$

$$I_4 = 2\pi N(1s) \sum_m a_m(1s) \lambda_{mk} \int \int dy y^2 D(\vec{r}_p, \vec{r}_1, \vec{r}_2) \times \left\{ \left(\frac{e^{-\mu_n r_p}}{\mu_n^3} + r_p \frac{e^{-\mu_n r_p}}{\mu_n^2} \right) r_p Y_{1m'}(\hat{r}_p) - \left(\frac{e^{-\mu_n r_2}}{\mu_n^3} + r_2 \frac{e^{-\mu_n r_2}}{\mu_n^2} \right) r_2 Y_{1m'}(\hat{r}_2) \right\} d\vec{r}_p d\vec{r}_1 d\vec{r}_2, \quad (\text{A6})$$

$$D \equiv \eta_{1s}(|\vec{r}_p - \vec{r}_2|) \eta_{1s}(|\vec{r}_p - \vec{r}_1|) \exp i \frac{1}{2} \vec{Q} \cdot \vec{r}_p \times \exp \left(-i \frac{1}{2} \vec{k}' \cdot \vec{r}_2 \right) \exp \left(i \frac{1}{2} \vec{k} \cdot \vec{r}_1 \right) u^+(\vec{r}_1) u_{1s}(\vec{r}_2). \quad (\text{A10})$$

where $\lambda_m = \beta_m + Z_n$ and $\lambda_{mk} = \beta_m + \delta_{2p}$.

β_m and δ_{2p} are the range parameters of the $1s$ and 2^1p states, respectively.

$$\mu_n = \lambda_{mk} \sqrt{y}, \quad (\text{A7})$$

$$A = 16\sqrt{2}\pi N(1s) \sum_{m=1}^2 a_m(1s) \frac{1}{\lambda_m^3}, \quad (\text{A8})$$

Now, integrals I_1 , I_2 , and I_3 are straightforward and given by Sarkar, Chaudhuri, and Ghosh [10]. Again in I_4 there are two terms, one can be obtained as a derivative of the other. $r_p^2 e^{-\mu_n r_p} Y_{1m}(\hat{r}_p)$ can be obtain from $r_p e^{-\mu_n r_p} Y_{1m}(\hat{r}_p)$ by taking the derivative of the latter with respect to μ_n . This is similar for the case in which r_p is replaced by r_2 . Hence, we are giving the expression for the two fundamental ones, i.e.,

$$I(r_p e^{-\mu_n r_p} Y_{1m}(\hat{r}_p)) \text{ and } I(r_2 e^{-\mu_n r_2} Y_{1m}(\hat{r}_2)).$$

Now, we present the integration results:

$$\begin{aligned} I(r_p e^{-\mu_n r_p} Y_{1m}(\hat{r}_p)) &= \int \exp \left(i \frac{1}{2} \vec{Q} \times \vec{r}_p \right) r_p \exp(-\mu_n r_p) Y_{1m}(\hat{r}_p) \omega^*(|\vec{r}_p - \vec{r}_2|) \omega(|\vec{r}_p - \vec{r}_1|) \\ &\quad \times \exp \left(-i \frac{1}{2} \vec{k}' \times \vec{r}_2 \right) \exp \left(i \frac{1}{2} \vec{k} \times \vec{r}_1 \right) u_{1s}(\vec{r}_2) u^+(\vec{r}_1) d\vec{r}_p d\vec{r}_1 d\vec{r}_2 \\ &= i32\pi\sqrt{2}\pi N_{1s} \alpha_i^2 Z_n \sum_m a_m(1s) \beta_m \int ds s(1-s) \int dp p(1-p) \\ &\quad \times \left(\frac{1}{\mu_1} \frac{\partial}{\partial \mu_1} \right)^2 \frac{1}{\mu_1} \left(\frac{1}{\mu_2} \frac{\partial}{\partial \mu_2} \right)^2 \frac{1}{\mu_2} \frac{\lambda}{(\rho^2 + \lambda^2)} \rho Y_{1m}(\hat{\rho}), \end{aligned} \quad (\text{A11})$$

where

$$\mu_1^2 = sZ_n^2 + (1-s)\alpha_i^2 + \frac{1}{4}s(1-s)k^2,$$

$$\mu_2^2 = p\beta_m^2 + (1-p)\alpha_i^2 + \frac{1}{4}p(1-p)k'^2,$$

(A12)

$$\vec{\rho} = \frac{1}{2} \{ (1+s)\vec{k} - (1+p)\vec{k}' \},$$

$$\lambda = \mu_n + \mu_1 + \mu_2.$$

$$\begin{aligned}
I(r_2 e^{-\mu_n r_2} Y_{1m}(\hat{r}_2)) &= \int \exp\left(i \frac{1}{2} \vec{Q} \cdot \vec{r}_p\right) r_2 \exp(-\mu_n r_2) Y_{1m}(\hat{r}_2) \omega^*(|\vec{r}_p - \vec{r}_2|) \omega(|\vec{r}_p - \vec{r}_1|) \\
&\quad \times \exp\left(-i \frac{1}{2} \vec{k}' \cdot \vec{r}_2\right) \exp\left(i \frac{1}{2} \vec{k} \cdot \vec{r}_1\right) u_{1s}(\vec{r}_2) u^+(\vec{r}_1) d\vec{r}_p d\vec{r}_1 d\vec{r}_2 \\
&= i 32 \pi \sqrt{2} \pi N_{1s} \alpha_i^2 Z_n \sum_m a_m(1s) \int ds s(1-s) \int dp p(1-p) \\
&\quad \times \left(\frac{1}{\mu_3} \frac{\partial}{\partial \mu_3}\right)^2 \left(\frac{1}{\mu_4} \frac{\partial}{\partial \mu_4}\right)^2 \frac{1}{\mu_4} \frac{\lambda_2}{(\rho_2^2 + \lambda_2^2)} \rho_2 Y_{1m}(\hat{\rho}_2), \tag{A13}
\end{aligned}$$

where

$$\begin{aligned}
\mu_3^2 &= s Z_n^2 + (1-s) \alpha_i^2 + \frac{1}{4} s(1-s) k^2, \\
\mu_4^2 &= p \mu_3^2 + (1-p) \alpha_i^2 + \frac{1}{4} p(1-p) \rho_3^2, \\
\vec{\rho}_3 &= \frac{1}{2} \{(1+s) \vec{k} - \vec{k}'\}, \\
\vec{\rho}_2 &= \frac{1}{2} \{p(1+s) \vec{k} - (1+p) \vec{k}'\}, \\
\lambda_2 &= \mu_n + \mu_3 + \beta_m.
\end{aligned} \tag{A14}$$

-
- [1] H. S. W. Massey and C. B. O. Mohr, Proc. Phys. Soc. London **67**, 695 (1954).
[2] P. A. Fraser, Proc. Phys. Soc. London **79**, 721 (1962).
[3] P. A. Fraser, J. Phys. B **1**, 1006 (1968).
[4] P. A. Fraser and M. Kraidy, Proc. Phys. Soc. London **89**, 533 (1966).
[5] M. I. Barker and B. H. Bransden, J. Phys. B **1**, 1109 (1968).
[6] M. I. Barker and B. H. Bransden, J. Phys. B **2**, 730 (1969).
[7] R. J. Drachman and S. K. Houston, J. Phys. B **3**, 1657 (1970).
[8] M. T. McAlinden, F. G. R. S. McDonald, and H. R. J. Walters, Can. J. Phys. **74**, 434 (1996).
[9] N. K. Sarkar and A. S. Ghosh, J. Phys. B **30**, 4591 (1997).
[10] N. K. Sarkar, P. Chaudhuri, and A. S. Ghosh, J. Phys. B **32**, 1657 (1999).
[11] J. E. Blackwood, C. P. Campbell, M. T. McAlinden, and H. R. J. Walters, Phys. Rev. A **60**, 4454 (1999).
[12] P. K. Biswas and S. K. Adhikari, Phys. Rev. A **59**, 363 (1999).
[13] G. Laricchia, M. Charlton, T. C. Griffith, and F. M. Jacobsen, in *Positron (Electron)-Gas Scattering*, edited by W. E. Kaupilla, T. S. Stein, and J. M. Wadhera (World Scientific, Singapore, 1986), p. 313.
[14] N. Zafar, G. Laricchia, M. Charlton, and A. Garner, Phys. Rev. Lett. **76**, 1595 (1996).
[15] A. J. Garner, G. Laricchia, and A. Qzen, J. Phys. B **29**, 5961 (1996).
[16] G. Laricchia, Hyperfine Interact. **100**, 71 (1996).
[17] A. J. Garner and G. Laricchia, Can. J. Phys. **74**, 518 (1996).
[18] A. J. Garner, A. Ozen, and G. Laricchia, Nucl. Instrum. Methods Phys. Res. B **143**, 155 (1998).
[19] Y. Nagashima, T. Hyodo, F. Fujiwara, and I. Ichimura, J. Phys. B **31**, 329 (1998).
[20] K. F. Canter, J. D. McNutt, and L. O. Roellig, Phys. Rev. A **12**, 375 (1975).
[21] P. G. Coleman, S. Rayner, F. M. Jacobsen, M. Charlton, and R. N. West, J. Phys. B **27**, 981 (1994).
[22] M. Skalsey, J. J. Engbrecht, R. K. Bithell, R. S. Vallery, and D. W. Gidley, Phys. Rev. Lett. **80**, 3727 (1998).
[23] H. Ray and A. S. Ghosh, J. Phys. B **31**, 4427 (1998).
[24] P. K. Sinha, A. Basu, and A. S. Ghosh, J. Phys. B **33**, 2579 (2000).
[25] A. Basu, P. K. Sinha, and A. S. Ghosh, Phys. Rev. A (to be published).
[26] G. Peach (unpublished), as quoted in Ref. [11] and Ref. [18].
[27] P. K. Sinha and A. S. Ghosh, Phys. Rev. A **58**, 242 (1998).
[28] T. G. Winter and C. C. Lin, Phys. Rev. A **12**, 434 (1975).
[29] A. S. Ghosh, A. Basu, T. K. Mukherjee, and P. K. Sinha, Phys. Rev. A (to be published).
[30] H. R. J. Walters (private communication).